Carcinogenesis, 2021, Vol. 42, No. 5, 772–783

doi:10.1093/carcin/bgab021
Advance Access publication March 12, 2021
Original Article

ORIGINAL ARTICLE

Host versus cell-dependent effects of β-arrestin 1 expression in prostate tumorigenesis

Timothy O.Adekoya, Nikia Smith, Ariel J.Thomas, Tonya S.Lane, Nija Burnette, Elizabeth J.Rivers, Yahui Li, Xiaoxin L.Chen[1] and Ricardo M.Richardson[1,*]

Julius L. Chambers Biomedical/Biotechnology Research Institute, North Carolina Central University, Durham, NC 27707, USA and [1]Department of Biological & Biomedical Sciences, North Carolina Central University, Durham, NC 27707, USA

*To whom correspondence should be addressed. Tel: 919-530-6421; Fax: 919-530-7780; Email: mrrichardson@nccu.edu

Abstract

Prostate cancer (PCa) constitutes a serious health challenge and remains one of the main causes of cancer-related death among men. The more aggressive form of the disease has been attributed to androgen independence, resulting in a lack of response to androgen deprivation therapy and sustained activation of other growth pathways. The scaffold proteins β-arrestin 1 and 2 (βarr1 and βarr2), which are known to mediate G protein-coupled receptor desensitization and internalization, were also shown to modulate prostate tumorigenesis. βarr1 is significantly overexpressed (>4-fold) in PCa cells relative to βarr2. In this study, we investigated the effect of βarr1 overexpression in PCa development and progression using the mouse and human PCa cell xenografts, and autochthonous transgenic adenocarcinoma of the mouse prostate (TRAMP) models deficient in β-arrestin depletion of βarr1 in TRAMP mice (TRAMP/βarr1$^{-/-}$) increased PCa growth and decreased overall survival relative to control TRAMP or TRAMP/βarr2$^{-/-}$ animals. Prostate tissues from TRAMP/βarr1$^{-/-}$ tumors displayed an increase in androgen receptor (AR) expression, whereas overexpression of βarr1 in TRAMP-C1 (TRAMP-C1-βarr1-GFP) which derived from TRAMP decreased AR expression, cell proliferation and tumor growth in nude mice xenografts, relative to control TRAMP-C1-GFP. Knockdown of βarr1 expression in human MDA PCa 2b cells (MDA PCa 2b-βarr1$^{-/-}$) also decreased AR expression cell proliferation and tumor growth relative to control (MDA PCa 2b-Sham) cells. Interestingly, both TRAMP-C1-βarr1-GFP and MDA PCa 2b-βarr1$^{-/-}$ xenografts showed a decrease in AKT phosphorylation but an increase in MAPK activation. Altogether, the data indicate that the effect of βarr1 in modulating AR signaling to regulate PCa aggressiveness is cell and host autonomous.

Introduction

Prostate cancer (PCa) is the most diagnosed cancer and the second leading cause of cancer-related deaths in American men (1). The widespread use of prostate-specific antigen (PSA) screening for PCa since the mid-1980s has increased the number of diagnoses (2). Fortunately, because PCa is now detected earlier, men are typically diagnosed with less severe disease. Since the localized disease is curable, early detection has significantly improved clinical outcomes (1–3). Despite these promising statistics, in the USA, being of African descent is a significant risk factor for having more severe disease (Gleason score >7) at diagnosis (3). Social and behavioral factors may account for some of the striking differences in PCa severity (4–6). Familial aggregation of PCa cases, however, supports the notion that development of PCa is, at least in part, due to genetic factors (7). Studies of the molecular mechanisms of PCa disparity have also revealed differences in androgen metabolism and inflammation (8,9). Although concentrations of testosterone and dihydrotestosterone (DHT) are similar within the prostate (10), African American males (AAM) tend to have higher systemic androgen levels and greater androgen receptor (AR) expression (10,11). AAM also expressed higher levels of proangiogenic chemokines which direct neovascularization of the growing tumor (9,12). In addition, the chemokine scavenger Duffy antigen receptor for

Received: January 15, 2021; **Revised:** February 24, 2021; **Accepted:** March 10, 2021

Abbreviations

AAM	African American men
AKT	protein kinase B
AR	androgen receptor
ERK	extracellular signal-regulated kinase
GPCR	G protein-coupled receptor
PSA	prostate serum antigen
TRAMP	transgenic adenocarcinoma of the mouse prostate
βarr1	β-arrestin 1
βarr2	β-arrestin 2

chemokines (DARC) was shown to be relatively absent in PCa of AAM (12). These observations implicate androgen metabolism, angiogenesis and inflammation in PCa progression and give possible underlying reasons for racial disparity.

Arrestins (Arr-1, Arr-2/βarr1, Arr-3/βarr2 and Arr-4) are a family of cytosolic proteins that regulate G protein-coupled receptor (GPCR) signaling following sustained stimulation with agonist, a process termed homologous desensitization (13–15). Arr-1 and Arr-4 are restricted to the visual system, whereas βarr1 and βarr2 are ubiquitously expressed (15). In addition to GPCRs downregulation, βarr1 and βarr2 are also involved in many important cellular functions including cell development, differentiation and chemotaxis (16,17). Several pathways critical to PCa converge at βarr1 and βarr2, including androgen metabolism, angiogenesis and metastasis (18,19). Knockdown of βarr1 in PCa cells was previously shown to decrease AR expression and activation, thereby inhibiting tumor development and metastasis (19). βarr2 was also shown to promote AR degradation resulting in loss of function and possibly, independence from AR signaling (18). This study was undertaken to determine *in vivo* the role of βarr1 overexpression in the onset of prostate adenocarcinoma. The data herein demonstrate that βarr1 overexpression may have opposite effect in PCa development, depending on the host or cell types.

Materials and methods

Materials

The PCa cell lines MDA PCa 2b (CRL-2422), PC3 (CRL-1435), LNCaP (CRL-1740), DU-145 (HTB-81), EOO6AA (CRL-3277) and TRAMP-C1 (CRL-2730), as well as the normal prostate cell line RWPE-1 (CRL-11609), were purchased from American Type Culture Collection (ATCC) (Manassas, VA). The cells were cytogenetically tested and authenticated using the short tandem repeat method before being frozen. All cell-based experiments were carried out on cells that have been tested and cultured for <12 weeks. Cell culture and molecular biology reagents, unless otherwise noted were purchased from Life Technologies (Carlsbad, CA). Human insulin (I9298), cholera toxin (C8052), phosphoethanolamine (P0503), hydrocortisone (H6909), selenious acid (211176), epidermal growth factor (EGF) (E4127), protease inhibitors cocktail (P8340), radioimmunoprecipitation assay (RIPA) buffer (R0278) and puromycin dihydrochloride (P9620) were purchased from Sigma–Aldrich (St. Louis, MO). RNeasy Mini Kit (74104) was purchased from Qiagen Inc. (Valencia, CA). XTT Cell Proliferation Assay Kit (30-1011K) was purchased from ATCC, whereas Geneticin (G418) (11811031), UltraPure LMP agarose (16520-050) and Lipofectamine 3000 (L3000-015) were purchased from Invitrogen. Plasmid transfection medium (sc-108062), UltraCruz transfection reagent (sc-395739), human βarr1 double nickase plasmid (sc-400642-NIC), βarr2 double nickase plasmid (sc-416686-NIC) and control double nickase plasmid (sc-437281) were obtained from Santa Cruz (Dallas, TX).

Nude (Nu/J) and transgenic adenocarcinoma of the mouse prostate (TRAMP C57BL/6) mice were purchased from The Jackson Laboratory (Bar Harbor, ME). βarr1$^{-/-}$ and βarr2$^{-/-}$ mice (C57BL/6) were a generous gift from Dr R. J. Lefkowitz (Duke University, Durham, NC). Extract-N-Amp Tissue PCR Kit was purchased from Sigma. βarr2 primers were synthesized by Invitrogen. βarr1 genotyping was performed by Transnetyx (Cordova, TN).

Development of TRAMP/βarr1$^{-/-}$ and TRAMP/βarr2$^{-/-}$ mouse models

All experiments and procedures were approved by and conformed to the guidelines of the Animal Care and Use Committee of North Carolina Central University, Durham, NC.

βarr1$^{-/-}$ or βarr2$^{-/-}$ (C57BL/6) mice were bred with TRAMP (C57BL/6) mice to generate TRAMP/βarr1$^{+/-}$ or TRAMP/βarr2$^{+/-}$ F1 generations. TRAMP/βarr1$^{+/-}$ or TRAMP/βarr2$^{+/-}$ mice were subsequently crossed with βarr1$^{-/-}$ or βarr2$^{-/-}$ mice, respectively, to maintain desired populations.

For genotyping, 1–2 cm sections of mouse tails were incubated at 55°C for 10 min, followed by 98°C for 3 min per manufacturer's protocol to extract DNA (Sigma). Nested primers that were used for βarr2 amplification are FL21 5′-TCTTCAAGAAGTCGAGCCCT-3′; FL22 5′-ACAGGGTCCACTTTGTCCA-3′; FL23 5′-GCTAAAGCGCATGCTCCAGA-3′. Primers used for TRAMP transgene SV40Tag were as follows: Forward 5′-CCGGTCGACCGGAAGCTTCCACAAGTGCATTTA-3′ and Reverse 5′-AGG CATTCCACCACTGCTCCCATTCATC-3′. Primers used for TRAMP transgene rPB CAT were: Forward 5′-GCGCTGCTGACTTTCTAAACATAAG-3′ and Reverse 5′-GAGCTCACGTTAAGTTTTGATGTGT-3′ (The Jackson Laboratory). PCR products were electrophoresed on 1% agarose gel for 40 min. βarr1 knockout animals can only be genotyped by Southern blotting (20). For accurate genotyping, mouse tails were sent to Transnetyx (Cordova, TN). By using real-time PCR, copy numbers of the βarr1 gene were determined to identify genotypes of TRAMP mice crossed with βarr1$^{-/-}$ animals.

Peritoneal recruitment of leukocytes

Zymosan was prepared in phosphate-buffered saline (PBS) to a final concentration of 1 mg/ml and 1.0 ml was injected into the peritoneum of control, βarr1- and βarr2-deficient mice. Mice were euthanized by CO_2 asphyxiation and the peritoneal cavity was lavaged at 4-h post-injection with 8 ml of ice-cold RPMI containing 2% FBS (fetal bovine serum) and 2 mM EDTA (ethylenediaminetetraacetic acid). Cells were collected by centrifugation, lysed and assayed for β-arrestin expression by western blotting.

Cell culture

MDA PCa 2b cells were cultured in Dulbecco's modified Eagle's medium (DMEM/Ham's F12) supplemented with 20% heat-inactivated FBS, 25 ng/ml cholera toxin, 10 ng/ml EGF, 0.005 mM phosphoethanolamine, 100 pg/ml hydrocortisone, 45 nM selenious acid, 0.005 mg/ml bovine or human insulin. LNCaP cells were cultured in RPMI 1640 supplemented with 10% FBS, 10 mM HEPES buffer, 1 mM sodium pyruvate, 1.26 g/L glucose, 100 μg/ml streptomycin and 100 IU/ml penicillin. PC3 cells were cultured in DMEM/Ham's F12 medium, supplemented with 10% FBS, 4 mM/L glutamine, 100 μg/ml streptomycin and 100 IU/ml penicillin. TRAMP-C1 cells were grown in DMEM supplemented with 5% FBS, 5% Nu-Serum IV, 10 nM dehydroisoandrosterone, 0.005 mg/ml bovine insulin, 1.5 g/L sodium bicarbonate, 100 μg/ml streptomycin and 100 IU/ml penicillin. Cell harvesting was performed using 0.05% Trypsin-EDTA (1×). All cells were maintained in a 5% CO_2 air atmosphere.

Knockout and overexpression of arrestins in PCa cell lines

To generate arrestin knockout in MDA PCa 2b cells, we utilized the double nickase gene-editing strategy (a D10A-mutated nickase version of CRISPR/Cas9). Cells (6×10^5) were initially seeded into a T-25 flask and allowed to fully attach over 2 days. Cells were then transfected with 6 μg of either βarr1 double nickase plasmid (sc-400642-NIC), βarr2 double nickase plasmid (sc-416686-NIC) or control (Sham) plasmid (sc-437281) using 18 μl UltraCruz transfection reagent and following protocol as instructed by the manufacturer (Santa Cruz). Twenty-four hours post-transfection, GFP (green fluorescent protein)-positive cells were sorted by flow cytometry and collected cells then placed under 1 μg/ml puromycin antibiotic selection for 5 days to obtain arrestin knockout clones as well as control (Sham) cells. Cells were assayed and subsequently used for further experiments. Assayed cells are a combined pool of at

least three independent selected clones and results validated by conducting knockout (along with corresponding control, Sham) on two separate occasions.

For overexpression of arrestins in LNCaP, PC3 and TRAMP-C1 cells, GFP-tagged arrestin constructs on pcDNA3.1 plasmids obtained from GenScript were utilized. Briefly, 4 × 10^6 cells were plated overnight in 100 mm^3 dishes. On the following day, cells were transfected with 40 µg plasmid containing enhanced GFP alone or GFP-tagged arrestin, using Lipofectamine 3000 as prescribed by the manufacturer. Twenty-four hours after transfection, cells were placed under selection using G418 antibiotic (1 mg/ml for both PC3 and LNCaP; 400 µg/ml for TRAMP-C1) for 4 weeks to obtain cells stably expressing proteins. Levels of mRNA transcripts and protein expression were monitored by real-time PCR and western blotting, respectively. Cells expressing GFP were later sorted by FACS and subsequently used for further experiments.

Real-time PCR

For βarr1 and βarr2 gene expression analysis, total RNA was extracted from cells following the manufacturer's protocol (Qiagen). RNA was diluted to a ratio of 1:1 with reverse transcriptase master mix (2×) and transcribed to cDNA. qRT-PCR was performed as described previously (20). Data are represented as fold change in mRNA expression. The experiments were repeated 3–4 times in triplicate.

Cell proliferation assay

Cell proliferation was determined as described previously (21). Briefly, adherent cells were harvested using trypsin and collected by centrifugation. Cells (1 × 10^4) were seeded in 100 µl of culture media per well in a 96-well plate and incubated overnight. Activated-XTT solution (50 µl) was added to cells in each well, and the plate was incubated in 5% CO_2 incubator at 37°C for 4 h before obtaining readings. Absorbance was measured at 490 nm using a spectrophotometer. Blank wells were used for background control.

Wound healing assay

For wound closure assay, 2 × 10^4 cells in 100 µl media were plated into each well of a 96-well ImageLock Microplate (Essen BioScience, Ann Arbor, MI, Cat #4379) and incubated overnight for TRAMP-C1 and 3 days for MDA PCa 2b cells. By using a 96-pin IncuCyte WoundMaker, the cell monolayer was gently scratched across the well and washed with growth media to remove cell debris. Fresh medium (100 µl) was then added, cells incubated and images of scratched wounds captured at different time points using the IncuCyte ZOOM® live-cell system (Essen BioScience, Ann Arbor, MI). Results were analyzed using the IncuCyte software and are presented as relative wound density.

Soft agar colony assay

As described previously for anchorage-independent growth in a 6-well plate (22), cells (5 × 10^3 per well) were suspended in 2 ml of 0.4% agar and plated on top of a solidified base layer containing 2 ml of 0.6% agar in complete growth media. Cultures were incubated at 37°C in 5% CO_2 incubator for 3 weeks, following which colonies were stained using 0.01% crystal violet solution. Colony images were captured using the Bio-Rad Gel Doc XR+ imaging system. Each experiment was performed in triplicates on two independent occasions.

Tumor xenografts

Male athymic nude mice (6–8 weeks) were injected subcutaneously with cells (5 × 10^6 cells/mice) resuspended in a 300 µl mix of growth media and matrigel (1.5:1 ratio). Tumor progression was monitored and measured over the course of the experiment. After 5–6 weeks, mice were euthanized by CO_2 asphyxiation. Tumors were dissected from mice, weighed and measured with a Thorpe Caliper. Tumor volume was calculated using the formula: $\text{Volume} = (d_1 \times d_2 \times d_3) \times 0.5236$ where d_n represents the three orthogonal diameter measurements (20). Tumor and tissue specimens were fixed in buffered formalin for further analysis.

Immunohistochemistry and semi-quantitation

Paraffin-embedded prostate tissue sections from TRAMP, TRAMP/βarr1$^{-/-}$ and TRAMP/βarr2$^{-/-}$ mice were dewaxed with xylene and rehydrated through graded series of alcohol. Tissue sections were treated with 0.10 M citric acid buffer in a heated pressure cooker for 10 min. Slides were blocked with normal goat serum and overlaid with 1:500 dilution of either control (rabbit), anti-βarr1, anti-βarr2 or anti-AR antibody overnight at 4°C. Slides were then rinsed and overlaid with secondary biotinylated goat anti-rabbit IgG (1:200) and incubated for 60 min. After washing with PBS, slides were overlaid with a 1:200 dilution of ExtrAvidin-peroxidase conjugate and incubated for 60 min. DAB (diaminobenzidine) was used for chromogenic localization of the antigen. After optimal color development, sections were washed with sterile water, counterstained with Mayer's hematoxylin and dehydrated into the graded series of alcohol and mounted.

FACS analysis of single-cell isolates from TRAMP tumors

Prostates were isolated from TRAMP mice (n = 3), minced with scissors to fine slurry and incubated in digestion buffer (RPMI 1640, 5% FBS, 1 mg/ml collagenase and 30 µg/ml DNase) at 37°C for 45 min. Single cells were washed, then cell counts and viability were determined using trypan blue exclusion on a hemocytometer. Cells (2 × 10^6) were resuspended in FACS analysis buffer and stained with PE (phycoerythrin)-conjugated anti-mouse CD3, CD4, CD45, CD8a, NKp46 or Ly6 antibodies. Stained cells were analyzed on a FACScan Flow Cytometer using CellQuest software. Unstained cells served as negative controls and were used to establish gating.

Immunoblotting

Rabbit βarr1/2 (4674S), βarr2 (3857S), GAPDH (2118S), anti-phospho-ERK ½ (4370S), anti-ERK ½ (9102S), anti-phospho-AKT (4058S) and anti-AKT (9272S) were obtained from Cell Signaling Technologies (Danvers, MA). Anti-AR (ab133273) and βarr1 rabbit monoclonal antibody (ab32099) were purchased from Abcam (Cambridge, MA), whereas anti-GFP (G1544), anti-mouse IgG (A9044) and anti-rabbit IgG (A9169) were obtained from Sigma–Aldrich.

For immunoblotting, cell pellets or minced tissues were washed and lysed in RIPA supplemented with a cocktail of protease inhibitor. Cell or tissue lysates were cleared by centrifugation for 10 min, protein estimated and 20–50 µg protein suspended in 4× loading buffer. Samples were boiled for 5 min and separated by SDS-PAGE. Resolved proteins were transferred into nitrocellulose paper and probed by using antibodies against the different proteins as indicated.

Statistical analyses

Results are expressed as mean ± SEM. Statistical analysis was performed using GraphPad Prism 5.0 (GraphPad Software, San Diego, CA). Differences between groups were determined using one-way ANOVA or Student's t-test (two-tailed), as appropriate. A P value <0.05 was considered statistically significant.

Results

Generation of TRAMP/βarr1$^{-/-}$ and TRAMP/βarr2$^{-/-}$ animal models

To assess *in vivo* the role of βarr1 and βarr2 in prostate tumor growth and metastasis, we used the well-established TRAMP model, in which an rPB-SV40 Tag transgene was constructed to generate transgenic mice from the C57BL/6 strain (23,24). These mice develop progressive PCa starting from mild hyperplasia at 8–12 weeks followed by severe hyperplasia, neoplasia and pulmonary and lymphatic metastatic cancer onset in 24–28 weeks (20, 24, 26). TRAMP mice were backcrossed with βarr1$^{-/-}$ or βarr2$^{-/-}$ mice, both of the C57BL/6 strain, to generate TRAMP/βarr1$^{-/-}$ and TRAMP/βarr2$^{-/-}$ populations. As shown in Figure 1A, TRAMP and βarr2 genes could be easily amplified using commercially

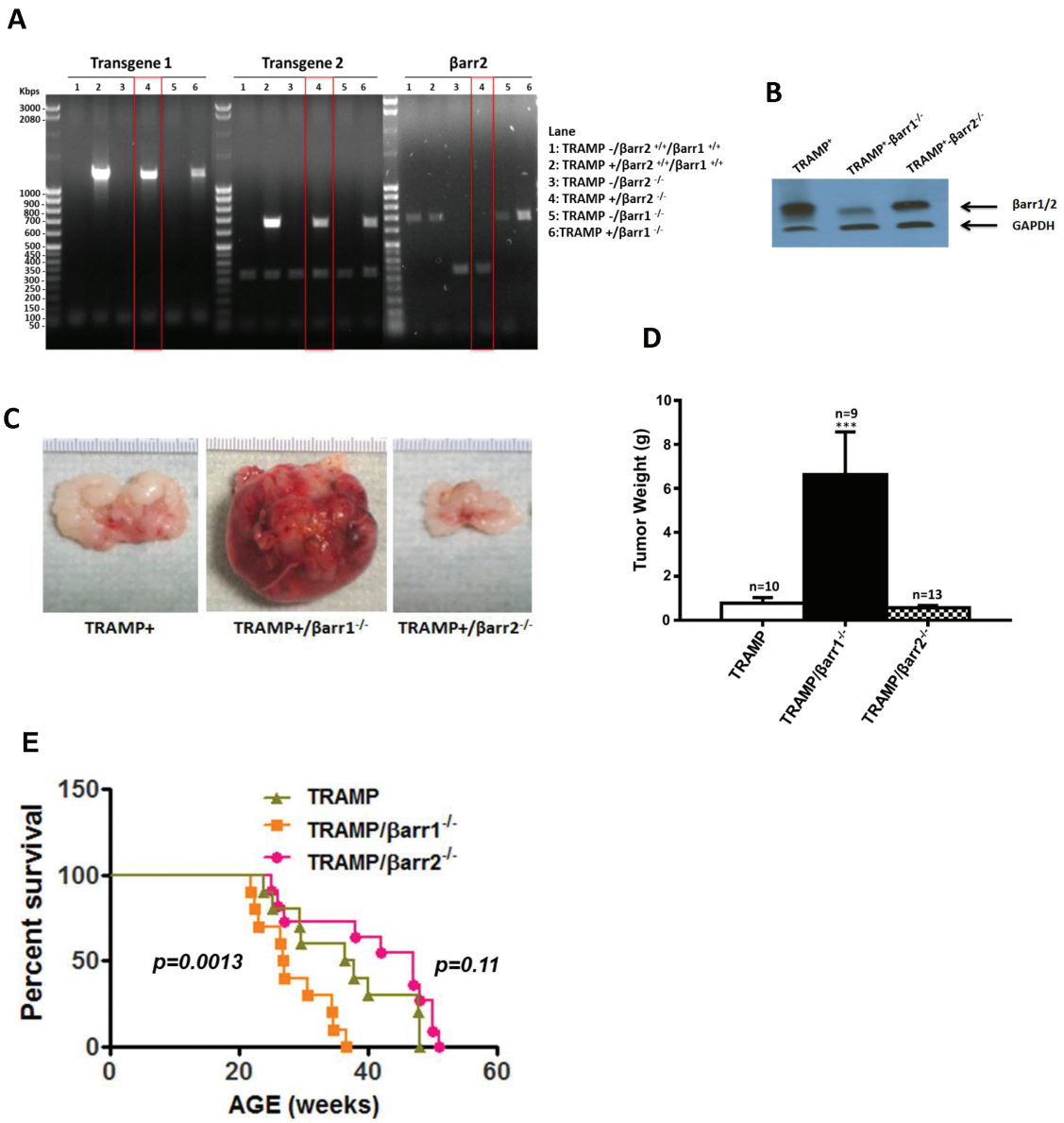

Figure 1. Tumor development in TRAMP, TRAMP/βarr1$^{-/-}$ and TRAMP/βarr2$^{-/-}$ mouse models. (**A**) Genotyping of TRAMP mice was performed by PCR using commercially available probes for the two transgenes as suggested by The Jackson laboratory. βarr2 genotyping was carried as described in Materials and methods. βarr1 genotyping was performed by Transnetyx. (**B**) βarr1 and βarr2 depletion were confirmed by immunoblotting using an anti-βarr1/βarr2 monoclonal antibody. Data shown are representative of 3 experiments. (**C**) Inhibition of βarr1 promotes prostate tumor development in TRAMP mice. Representative PCa in TRAMP, TRAMP/βarr1$^{-/-}$ and TRAMP/βarr2$^{-/-}$ mice after 30 weeks. (**D**) Average tumor weight after 30 weeks. ***$P < 0.001$. (**E**) For survival rate, TRAMP ($n = 12$), TRAMP/βarr1$^{-/-}$ ($n = 10$) and TRAMP/βarr2$^{-/-}$ ($n = 12$) were kept in observation up to 55 weeks for mortality. Survival based on natural death or point at which tumors grew to become too large was determined. The experiments were repeated twice with similar results.

available primers. Genotyping of βarr1$^{-/-}$ mice was carried out by Southern blotting or by Transnetyx, an automated genotyping service. To further confirm the genotyping results, cell lysates were assayed by western blotting for βarr1 and βarr2 expression using a βarr1/2 antibody. As shown in Figure 1B and Supplementary Figure S3, TRAMP displayed expression of both βarr1 and βarr2 whereas TRAMP/βarr1$^{-/-}$ (middle lane) and TRAMP/βarr2$^{-/-}$ (right lane) were deficient in βarr1 or βarr2 expression, respectively.

TRAMP, TRAMP/βarr1$^{-/-}$ and TRAMP/βarr2$^{-/-}$ animals were observed for 30 weeks for the onset and progression of orthotopic tumors (Figure 1C). Tumors from TRAMP/βarr1$^{-/-}$ animals were 8 times (6.64 ± 1.94 g) the weight of TRAMP (0.78 ± 0.26 g) tumors (Figure 1C, left versus center panel; Figure 1D). The averaged tumors from TRAMP/βarr2$^{-/-}$ mice were similar to that of control TRAMP (0.58 ± 0.11 g; Figure 1C and D).

We next determine the effect of β-arrestin deficiency on TRAMP mouse survival. As shown in Figure 1E, βarr1 deletion caused a significant ($P = 0.0013$) reduction in the median survival of TRAMP/βarr1$^{-/-}$ mice (~38 weeks) relative to control TRAMP mice (~44 weeks). TRAMP/βarr2$^{-/-}$ animals displayed a slight but not significant increase (~46 weeks) in the median survival.

Effect of βarr1 depletion on intratumor leukocytes infiltration

We next analyzed the intratumor leukocyte infiltration of cell isolates from prostate tumors of TRAMP^{+} and TRAMP^{+}/βarr1$^{-/-}$ mice. As shown in Figure 2, a significant decrease was observed in

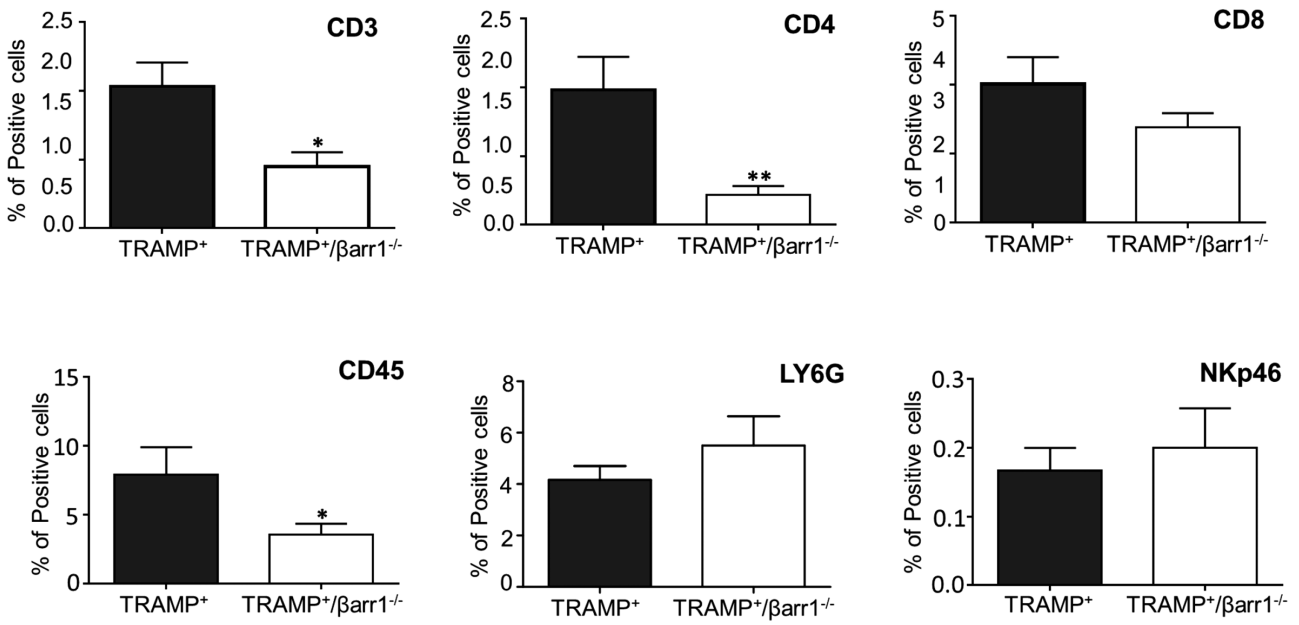

Figure 2. FACS analysis of intratumor-infiltrating leukocyte subpopulations. Single-cell isolates from TRAMP and TRAMP/βarr1$^{-/-}$ prostate tumors (n = 3) were stained for different leukocyte subpopulations: CD3, CD4, CD8, CD45, LY6G and NKp46 and were analyzed by a FACScan flow cytometer using CellQuest software. *$P < 0.05$; **$P < 0.01$.

tumor-infiltrating CD3$^+$, CD4$^+$, CD8$^+$ and CD45$^+$ in TRAMP$^+$/βarr1$^{-/-}$ as compared with TRAMP$^+$ mice. No significant difference was found in tumor-infiltrating polymorphonuclear or natural killer cells as determined by Ly6G and NKp46 staining, respectively.

Overexpression of βarr1 in TRAMP-C1 cells inhibited tumor growth

To further investigate the effect of βarr1 in tumor progression, we used the TRAMP-C1 tumorigenic cell line that was established from the TRAMP mouse model (27). Western blot analysis revealed a lower expression of βarr1 in TRAMP-C1 cells as compared with the human PCa cell lines LNCaP (~20-fold), PC3 (~10-fold) and MDA PCa 2b (~40-fold) (Figure 3A and Supplementary Figure S1, available at *Carcinogenesis* Online). A pcDNA3 vector expressing a GFP tag at the C-terminus was used to generate TRAMP-C1 cells stably overexpressing βarr1 (TRAMP-C1-βarr1-GFP) or GFP alone (TRAMP-C1-GFP). βarr1 overexpression was confirmed by western blotting using both βarr1- (Figure 3B) and GFP (data not shown)-specific antibodies. TRAMP-C1-βarr1-GFP cells displayed significant decrease in cell migration (Figure 3C and D) and anchorage-independent cell growth in soft agar (Figure 3E), relative to TRAMP-C1-GFP or control TRAMP-C1 cells.

Xenografts in nude mice were used to assess the effect of βarr1 overexpression in TRAMP-C1 cell tumor development. Nude mice (n = 5) of 6–8 weeks of age were injected with (5 × 10^6) control TRAMP-C1-GFP or TRAMP-C1-βarr1-GFP cells. Heterotopic tumor growth was monitored and tumor volume was measured. As shown in Figure 3F, TRAMP-C1-βarr1-GFP cells developed significantly smaller tumor xenografts (0.04 ± 0.0182 g) as compared with TRAMP-C1-GFP (0.102 ± 0.0132) cells. These data support the ones obtained with TRAMP/βarr1$^{-/-}$ mouse model and indicate that βarr1 expression in the TRAMP system may delay the onset of PCa.

βarr1 knockdown in MDA PCa 2b cells inhibited tumor growth

It was previously shown that βarr1 inhibition in human PCa cells decreased tumor growth (19). These data contrasted with the ones obtained with the TRAMP/βarr1$^{-/-}$ mouse model or TRAMP-C1 cells overexpressing βarr1 (Figures 1 and 3F). To further assess the effect of βarr1 in PCa tumorigenesis, we inhibited both βarr1 and βarr2 expression in the human MDA PCa 2b cell line, using CRISPR double nickase plasmids with either Sham vector or vector containing βarr1- or βarr2-specific targets. Stable cell lines deficient in βarr1 (MDA PCa 2b-βarr1$^{-/-}$) or βarr2 (MDA PCa 2b-βarr2$^{-/-}$) were generated and analyzed. As shown in Figure 4A, expression of βarr1 and βarr2 was reduced by ~98% in both MDA PCa 2b-βarr1$^{-/-}$ and MDA PCa 2b-βarr2$^{-/-}$. MDA PCa 2b-βarr1$^{-/-}$ cells exhibited significant decrease in cell proliferation (Figure 4B), cell migration (Figure 4C and D) and anchorage-independent cell growth in soft agar (Figure 4E), relative to MDA PCa 2b-βarr2$^{-/-}$ or MDA PCa 2b expressing the vector alone (MDA PCa 2b-Sham).

Tumor xenografts in nude mice (Figure 4F) also demonstrated that MDA PCa 2b-βarr1$^{-/-}$ mice developed significantly smaller tumors (1.28 ± 0.34 g) relative to control MDA PCa 2b-Sham (4.71 ± 0.37 g). MDA PCa 2b-βarr2$^{-/-}$ showed a slight but not significant difference in tumor volume and weight (3.25 ± 0.52 g) relative to control. These data confirm a previously published report using LNCaP and C4-2 cells deficient in βarr1 expression (19), but differ from that of TRAMP-βarr1$^{-/-}$ animals (Figure 1) but mirrored the ones obtained with TRAMP-C1-βarr1-GFP cells (Figure 3).

Overexpression of βarr2 in LNCaP and PC3 cells showed no significant difference in tumor growth, relative to control cells expressing the vector alone (Supplementary Figure S2A and B, available at *Carcinogenesis* Online).

Effects of βarr1 deletion on tumor expression of AR and prostate serum antigen

The effect of βarr1 depletion on prostate tissue from TRAMP animals was also analyzed by histological examination of tumors from TRAMP and TRAMP/βarr1$^{-/-}$ mice, using murine AR. As shown in Figure 5A, TRAMP/βarr1$^{-/-}$ prostate showed a marked increase in AR expression as compared with

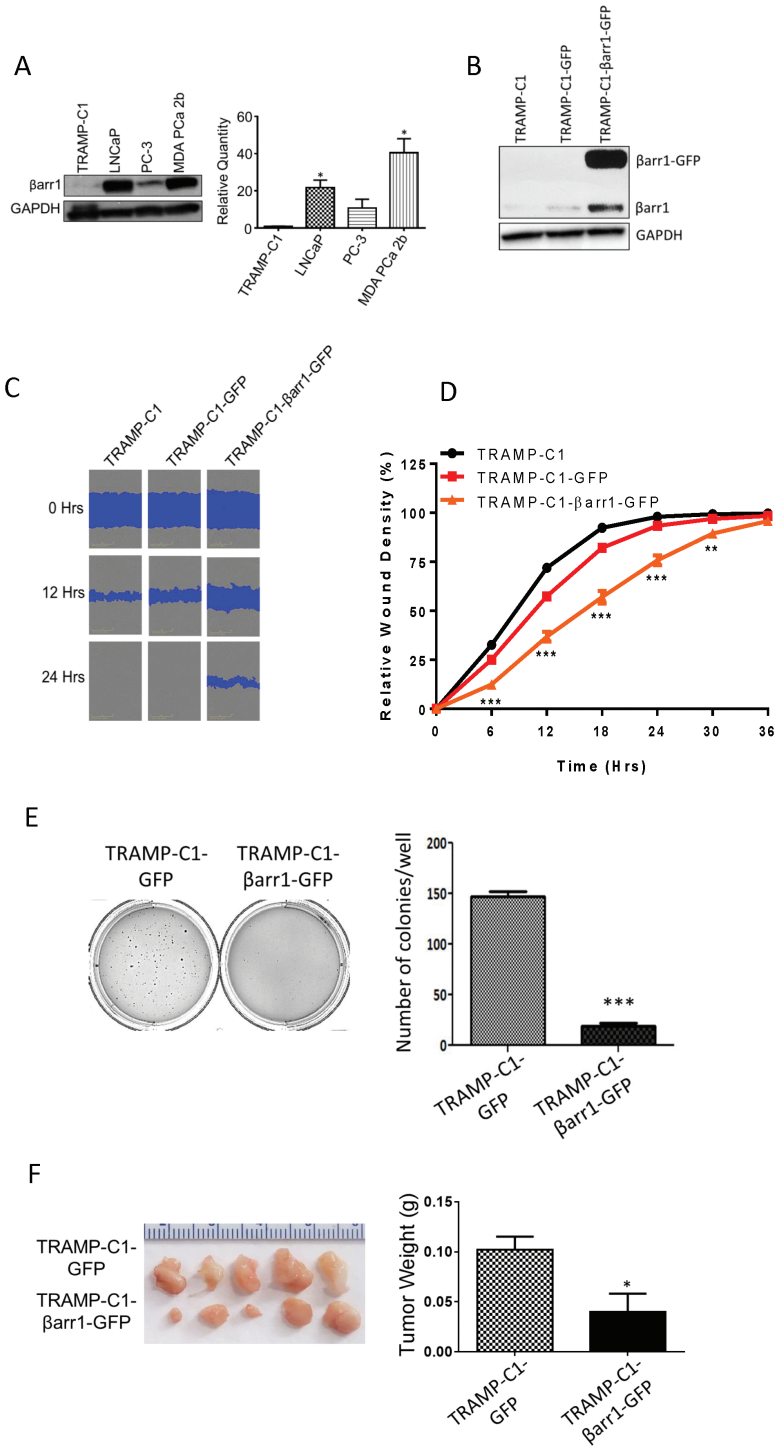

Figure 3. Overexpression of βarr1 in TRAMP-C1 cells inhibits cell proliferation and tumor growth. (**A**) Western blotting analysis of βarr1 expression in TRAMP-C1 cells relative to LNCaP, PC3 and MDA PCa 2b cells. Band density was calculated by ImageJ software, normalized for GAPDH expression and are the averages of three experiments. (**B**) Overexpression of βarr1 in TRAMP-C1 cells using a pcDNA3 plasmid containing a GFP-tagged βarr1 (TRAMP-C1-βarr1-GFP) or vector alone (TRAMP-C1-GFP). G418-resistant cells were selected and analyzed by immunoblotting using anti-βarr1 or anti-GFP. (**C**) For cell migration assays, closure of the wound was continuously monitored using the IncuCyte system until scratches were closed. Data shown are the representative image of wound healing assay at 0, 12 and 24 h. (**D**) Graphical quantification of the rate of wound closure expressed as relative wound density (%). Data shown are representative of two experiments performed in sextuplicates. (**E**) Colony formation assay was used to determine anchorage-independent cell growth of TRAMP-C1-βarr1-GFP or control TRAMP-C1-GFP cells. Representative images and graphical quantification of number of colonies were determined after 21 days. (**F**) For tumor xenografts, cells (5×10^6 cells) were injected subcutaneously into 6- to 8-week-old nude mice. Mice were euthanized and tumor weight was determined after 6 weeks. Representative images of dissected tumors and normalized tumor weight are shown. The results are representative of one of the three experiments. $^*P < 0.05$, $^{**}P < 0.01$, $^{***}P < 0.001$.

control TRAMP prostate. Tumor lysates were also assayed by western blotting and showed a ~4-fold increase (3.8 ± 0.48) in AR expression as compared with TRAMP (Figure 5B and C). Tumors xenografts from TRAMP-C1 cells overexpressing βarr1 (TRAMP-C1-βarr1-GFP) exhibited a significant decrease in AR (42.95 ± 8.74) relative to control TRAMP-C1-GFP cells (100 ± 10.98) (Figure 5D and E).

We next assessed the effect of βarr1 deletion in AR and PSA expression in MDA PCa 2b tumor xenografts. As shown in Figure 5F and G, MDA PCa 2b-βarr1$^{-/-}$ tumors displayed ~80% decrease in AR expression (20.59 ± 1.65) relative to tumors from MDA PCa 2b-Sham cells (100 ± 9.85). In contrast, PSA expression in MDA PCa 2b-βarr1$^{-/-}$ tumors increased ~2.3-fold (229.10 ± 13.61) relative to MDA PCa 2b-Sham (100 ± 8.00) tumors (Figure 5F and H).

Effects of βarr1 in AKT and MAPK activation

To determine the effect of βarr1 expression in AKT and MAPK expression and activation, prostate lysates from TRAMP and TRAMP/βarr1$^{-/-}$ mice were assayed for total AKT and ERK as well as phospho-AKT (p-AKT) and phospho-ERK (p-ERK). TRAMP/βarr1$^{-/-}$ tumors showed a ~3-fold increase in AKT expression (304 ± 21) relative to GAPDH, as compared with TRAMP (100 ± 29) (Figure 6A and B). The increase in AKT expression in TRAMP/βarr1$^{-/-}$ tumors, however, correlated with a significant decrease in AKT phosphorylation (21.35 ± 9) as compared with TRAMP (100 ± 3.3) (Figure 6A and C). No significant difference was found in ERK expression relative to GAPDH (100 ± 27 and 87 ± 20 for TRAMP/βarr1$^{-/-}$ and TRAMP, respectively; Figure 5A and D). ERK activation, however, decreased by ~40% in TRAMP/βarr1$^{-/-}$ (63 ± 2.3) as compared with TRAMP (100 ± 0.1) Figure 5A and E).

We next assayed TRAMP-C1-βarr1-GFP and TRAMP-C1-GFP tumor xenograft lysates for total and phosphorylated AKT and ERK. No significant difference in AKT and ERK expression was detected in TRAMP-C1-βarr1-GFP relative to control TRAMP-C1-GFP tumors (Figure 6F). TRAMP-C1-βarr1-GFP displayed a significant decrease in AKT (37.04 ± 6.02; Figure 6F and G) but an increase in ERK (166.70 ± 14.2, Figure 6F and H) phosphorylation, as compared with TRAMP-C1-GFP (100 ± 1.85 and 100 ± 6.29, respectively; Figure 6F–H).

Tumor xenografts from MDA PCa 2b-βarr1$^{-/-}$ also displayed decrease in AKT (45.06 ± 11.64; Figure 6I and J) and increase in ERK (159.4 ± 4.84, Figure 6I, G and K) activation relative to control MDA PCa 2b-Sham (100 ± 13.42 and 100 ± 13.70, respectively; Figure 6I–K).

Discussion

PCa is a well-studied disease, but yet there are still many unknowns with regard to the onset, progression and metastatic aspects of prostate tumorigenesis (28). In addition, the eventual transformation from androgen dependent to the more aggressive form of androgen-independent or castration-resistant PCa has further complicated the molecular understanding of the disease. Several recent studies have shown that in addition to GPCR desensitization and downregulation, β-arrestins regulate AR expression and functions thereby modulating PCa development and prognosis (18,19). βarr1 was shown to be overexpressed (4- to 40-fold) in most PCa cell lines relative to βarr2 (Supplementary Figure S1, available at *Carcinogenesis* Online). To investigate *in vivo* the role of βarr1 overexpression in prostate tumorigenesis, we used the well-established TRAMP mouse model of PCa to generate βarr1-deficient (TRAMP/βarr1$^{-/-}$) and βarr2-deficient (TRAMP/βarr2$^{-/-}$) TRAMP models. The data herein indicate that the effect of βarr1 in PCa development and progression may be host-dependent. First, TRAMP/βarr1$^{-/-}$ animals showed aggressive tumor growth and significantly lower survival rate relative to control TRAMP or TRAMP/βarr2$^{-/-}$ mice. Second, overexpression of βarr1 in the murine TRAMP-C1 cells which were derived from the TRAMP prostate, decreased cell proliferation and tumor growth in nude mice relative to control TRAMP-C1 cells (Figure 3). In contrast, knockout of βarr1 expression in human MDA PCa 2b cells, decreased cell proliferation and xenograft tumor growth in nude mice (Figure 4).

The infiltration of immune cells into tumor microenvironment (TME) is a key component of the tumor immunity (29). Tumor from TRAMP/βarr1$^{-/-}$ model displayed significant decrease in tumor-infiltrating lymphocytes (TILs) including CD4, CD8, CD3 and CD45, in the TME relative to TRAMP or TRAMP/βarr2$^{-/-}$ mice (Figure 2, data not shown). The decrease of TILs in TRAMP/βarr1$^{-/-}$ mice tumors could be due to defective leukocyte migration caused by the lack of βarr1/cytoskeleton molecules scaffolding properties or suppressed the release of chemoattractive cytokines by the tumor cells (30). Nevertheless, whether this decrease in T-cell infiltration alone contributes to the significant difference in tumor development and survival of TRAMP/βarr1$^{-/-}$ mice remains to be investigated. Elevated levels of T lymphocytes in tumor infiltrates, however, have been associated with better prognosis due to their antitumor immune responses (31). Yang *et al.* (32) recently reported that high intratumoral CD8+ T-cell infiltration is associated with improved survival in PCa patients undergoing radical prostatectomy.

It was previously reported that βarr1 expression in PCa cells correlates with AR expression and activation (19). Inhibition of βarr1 in the castration-resistant PCa line C2-4 and to a lesser extent, the androgen-dependent LNCaP cells were shown to decrease AR expression thereby suppressing tumor progression and metastasis (19). Immunohistochemical and immunoblotting analysis of prostate tissues from TRAMP/βarr1$^{-/-}$ animals, however, revealed a marked increase in AR expression and nuclear localization (Figure 5A–C). The reason for this discrepancy remains unclear. AR overexpression, however, has been correlated to both tumor suppression and tumor progression (33). Thus, it could be that in the TRAMP mouse model, the axis AR/βarr1 functions as a tumor suppressor. Supporting this contention is that overexpression of βarr1 in TRAMP-C1 cells, which were derived from TRAMP prostate adenocarcinoma, reversed the effect of βarr1 inhibition, resulting in a significant decrease of AR expression, cell proliferation, colony formation and xenografts tumor growth (Figures 3, 5D and E). AR has also been shown to interact with a large number (>300) of cofactors to regulate its gene transcriptional activity (34,35). Another explanation could be that in the TRAMP model, AR couples to different cofactors to modulate prostate tumorigenesis. Indeed, as was the case for C2-4 and LNCaP cells (19), CRISPR knockout of βarr1 in the human MDA PCa 2b cell line decreased AR expression, cell proliferation and tumor growth (Figures 4, 5F and G).

AR inhibition in MDA PCa 2b xenografts correlated with an increase in PSA expression (Figure 5F and H). Several studies have previously reported the existence of alternative AR-independent pathways for the control of PSA expression (36). Indeed, several transcription factors, including GAGATA-binding protein, epithelium-specific Ets factor 2 (ESE2) and prostate-derived Ets factor (PDEF), have been shown to induce PSA expression independently of AR activation (37–39). In addition, nuclear βarr1 was recently shown to directly interact with a large number of genes, including AR, to modulate their transcriptional activity (19,40). Thus, it could be that the loss of the βarr1/AR regulatory mechanism promoted the effect(s) of other coactivators of androgen-dependent genes, thereby increasing the expression of PSA.

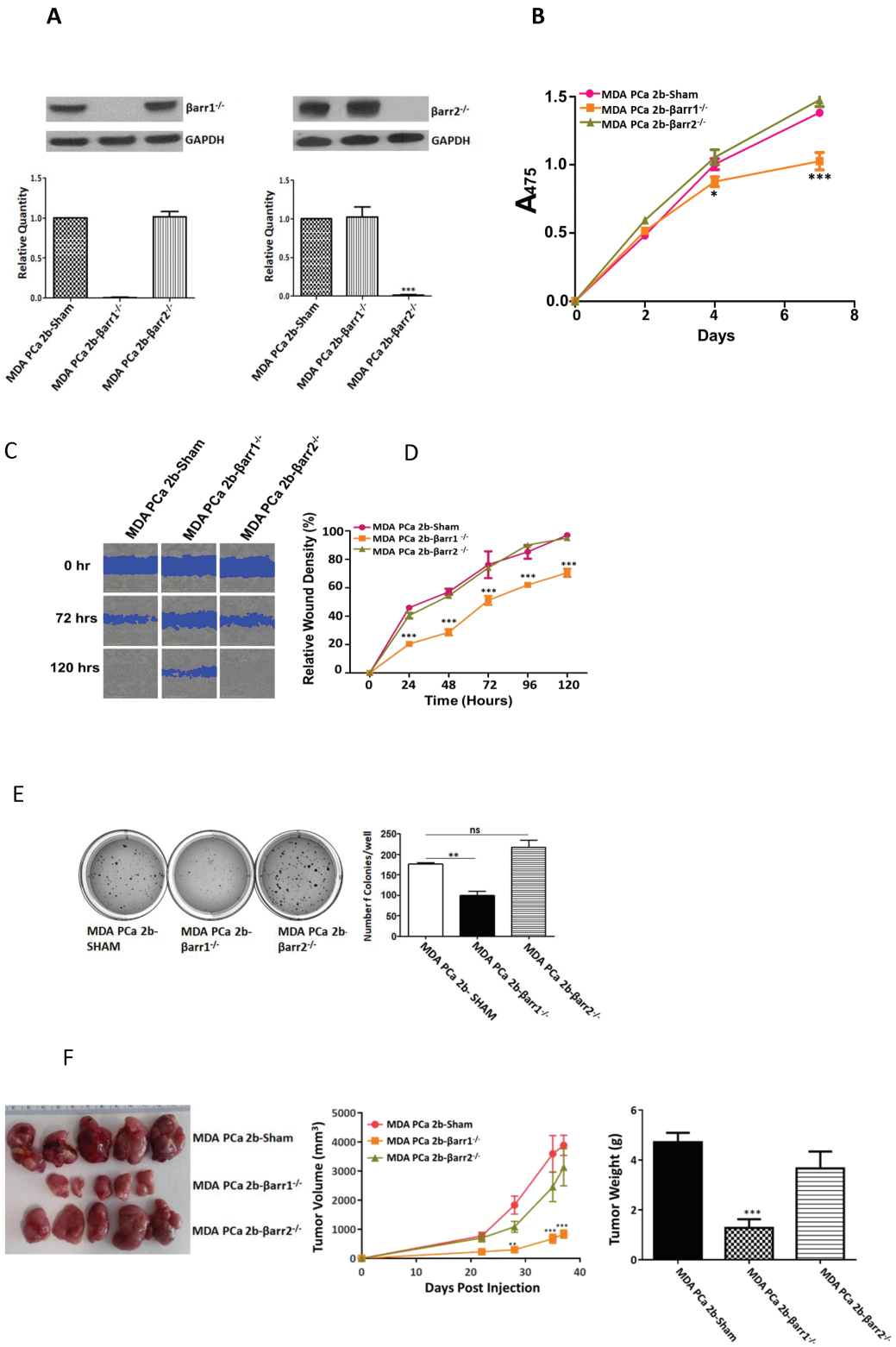

Figure 4. Knockdown of βarr1 in MDA PCa 2b cells inhibits cell proliferation and tumor growth. MDA PCa 2b cells were transfected with CRISPR double nickase plasmids containing targets specific for βarr1 (MDA PCa 2b βarr1$^{-/-}$) or βarr2 (MDA PCa 2b βarr2$^{-/-}$). Puromycin-resistant cells were selected and analyzed by immunoblotting using anti-βarr1 or anti-βarr-2 antibodies. (**A**) Data shown are representative of three experiments. ***P < 0.001. (**B**) Cell proliferation study of MDA PCa 2b-Sham, MDA PCa 2b βarr1$^{-/-}$ and MDA PCa 2b βarr2$^{-/-}$ cells were carried out as described in Materials and methods. Data are expressed as fold change in absorbance at 490 nm over time and are an average from four independent experiments. *P < 0.05; ***P < 0.001. (**C**) For cell migration assays, closure of wound was continuously monitored using the IncuCyte system, until scratches were closed. Data shown are the representative image of wound healing assay at 0, 72 and 120 h. (**D**) Graphical quantification of the rate of wound closure expressed as relative wound density (%). Data shown are representative of two experiments performed in sextuplicates. (**E**) Colony formation assay was used to determine anchorage-independent cell growth of control MDA PCa 2b-Sham, MDA PCa 2b βarr1$^{-/-}$ and MDA PCa 2b βarr2$^{-/-}$ cells. Representative images and graphical quantification of the number of colonies were determined after 21 days. (**F**) For tumor xenografts, cells (5 × 10^6 cells) were injected subcutaneously into 6- to 8-week-old nude mice, and tumor volume was measured weekly. Mice were euthanized and tumor weight was determined after 6 weeks. Representative images of dissected tumors, tumor volume over time and tumor weight are shown. The results are representative of one of the three experiments. **P < 0.01, ***P < 0.001.

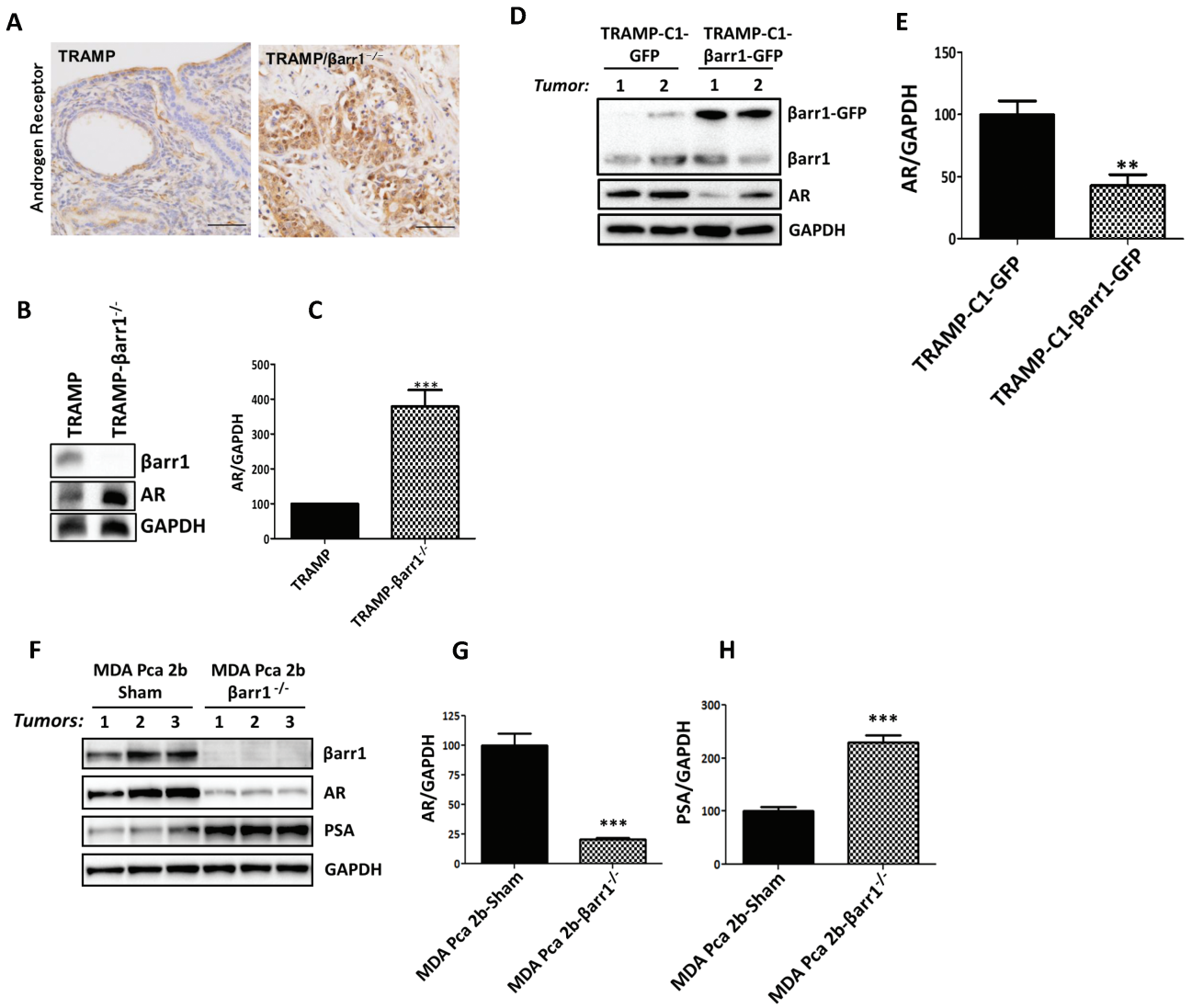

Figure 5. Effect of βarr1 expression in AR activity. (**A**) Tissue from TRAMP and TRAMP/βarr1$^{-/-}$ prostate tumors were immunostained with anti-AR antibody. Representative images of two independent experiments are shown. Scale bars: 50 μm. (**B**, **C**) Tumor lysates from TRAMP and TRAMP/βarr1$^{-/-}$ were minced, lysed in RIPA and 40 μg of proteins were resolved in 10% SDS-PAGE and analyzed by western blotting for βarr1 and AR expression. Representative image (B) and graphical representation of AR band densities relative to GAPDH (C) from three experiments are shown. ***$P < 0.001$. (**D**) Tumor xenografts from TRAMP-C1-βarr1-GFP and TRAMP-C1-Sham lysed in RIPA and analyzed by western blotting for βarr1 and AR expression. (**E**) Graphical representation of AR band densities from western blots, relative to GAPDH. Data shown are representative of three experiments. **$P < 0.01$. (**F**) MDA PCa 2b βarr1$^{-/-}$ and MDA PCa 2b-Sham tumors from nude mice were lysed as described above and assayed for AR and PSA expression. (**G**, **H**) Graphical representation of band densities from western blots, relative to GAPDH. Data shown are representative of four experiments. ***$P < 0.001$.

Kong *et al.* (41) recently reported that βarr1 overexpression in PC3 and DU-145 modulates tumor progression via an AKT/ERK-dependent pathway. The data herein, however, demonstrated that alteration of the axis βarr1/AR in tumor xenografts by either overexpression (TRAMP C1-βarr1-GFP) or depletion (MDA PCa 2b-βarr1$^{-/-}$) of βarr1, correlated with increase ERK phosphorylation but decrease AKT activation (Figure 6), cell migration and tumor progression (Figures 3 and 4). Both reciprocal and inverse correlation between AKT activation and members of the MAPK family, including p38 MAPK and ERK has been previously reported in prostate tumorigenesis (42–44). Malik *et al.* (44) have shown that advanced PCa correlates with increased AKT but decreased ERK activation. Gioeli *et al.* (45), however, reported a direct correlation between ERK activation and Gleason score in prostate tissues. Similarly, tumor lysates from TRAMP/βarr1$^{-/-}$ animals displayed decreased activation of both AKT and ERK, despite a 3-fold increase in AKT expression, relative to TRAMP (Figure 6A–E). These data further underscore the variability of βarr1 functions in prostate tumorigenesis, which may be cell- and host-dependent.

β-arrestins are also known to modulate GPCRs-mediated downstream effectors activation, including MAPK and PI3K, to regulate cellular functions. Multiple studies have reported varying expression levels of several GPCRs among PCa cell lines (46,47). Thus, it could be that the alternate modulatory effects of βarr1/AR observed between the TRAMP-C1 and MDA PCa 2b cell lines are due to differential expression pattern of certain GPCRs between these cells.

A previous study using prostatectomy samples revealed a negative correlation between βarr2 and AR expression (18). Inhibition of βarr2 in LNCaP cells was shown to increase AR activity and PSA expression (18). Depletion of βarr2 expression in

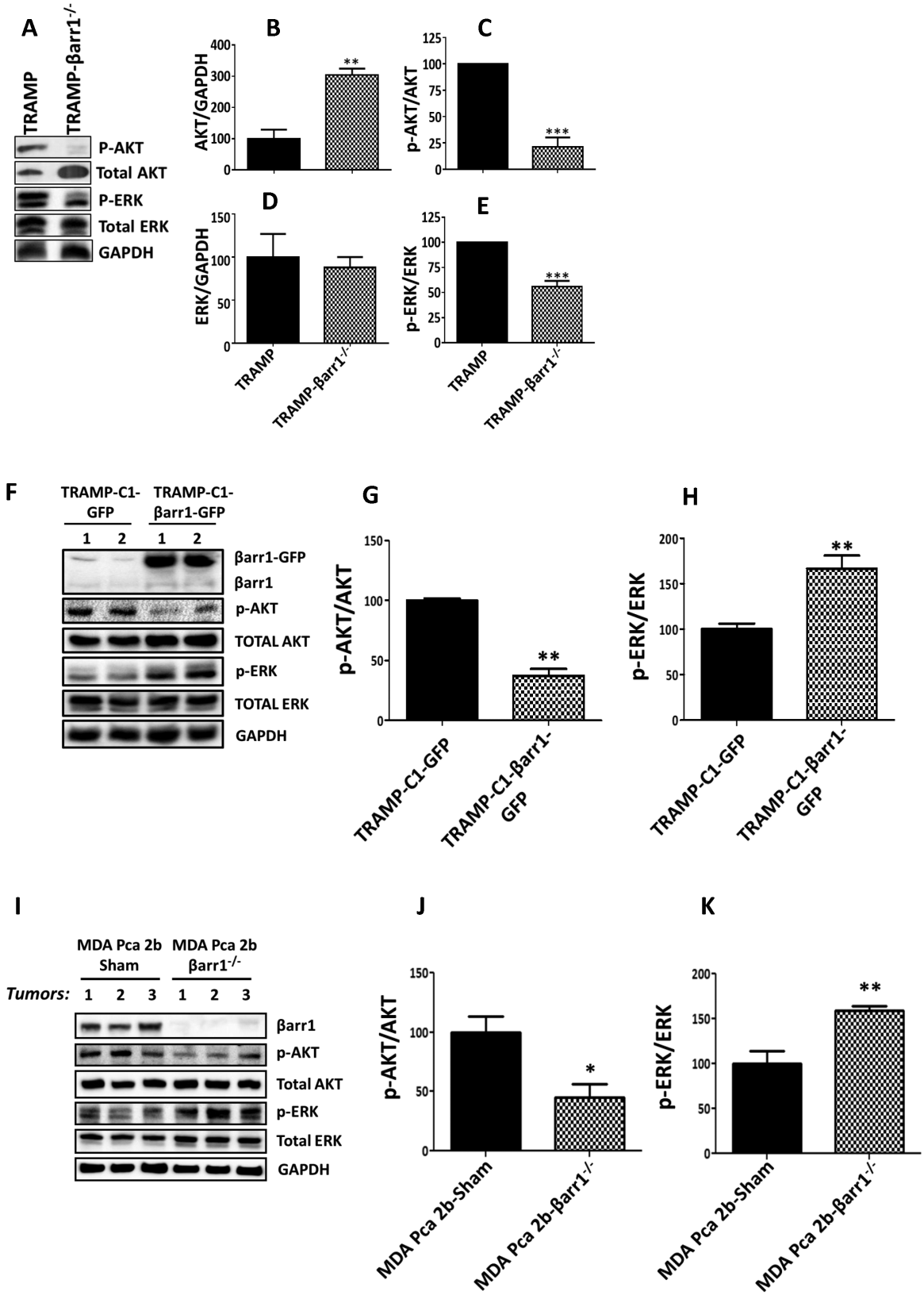

Figure 6. Effect of βarr1 on AKT and ERK activation. (**A**) Tumor lysates from TRAMP and TRAMP/βarr1$^{-/-}$ were lysed in RIPA and 40 μg of proteins were analyzed by western blotting for βarr1, AKT, p-AKT, ERK, p-ERK and GAPDH. Graphical representation of band densities of AKT (**B**) and ERK (**D**) relative to GAPDH as well as phospho-AKT (**C**) and phospho-ERK (**E**) relative to total AKT and ERK, respectively. (**F**) TRAMP-C1-βarr1-GFP and TRAMP-C1-Sham lysates were immunoblotted and assayed for βarr1, AKT, p-AKT, ERK, p-ERK and GAPDH. Graphical representation of band densities of p-AKT (**G**) and pERK (**H**) relative to total AKT and total ERK, respectively. Data shown are from four different experiments. $^{**}P < 0.01$. (**I**) MDA PCa 2b βarr1$^{-/-}$ and MDA PCa 2b-Sham tumor lysates were assayed by western blotting for βarr1, AKT, p-AKT, ERK, p-ERK and GAPDH. Graphical representation of band densities of p-AKT (**J**) and pERK (**K**) relative to total AKT and total ERK, respectively. Data shown are representative of two experiments. $^{*}P < 0.05$, $^{**}P < 0.01$.

both TRAMP mice (TRAMP/βarr2$^{-/-}$; Figure 1 and Supplementary Figure S3) and MDA PCa 2b cells (MDA PCa 2b/βarr2$^{-/-}$; Figure 4) showed no significant effect in cell proliferation or tumor development compared with control cell (MDA PCa 2b-Sham) or animal (TRAMP). In addition, overexpression of βarr2 in both LNCaP and PC3 cells also showed no significant effect in tumor growth (Supplementary Figure S2, available at *Carcinogenesis* Online).

In summary, the data herein have shown that βarr1 expression modulates prostate tumor development and prognosis. The ability to suppress or promote tumor growth may depend on several factors including animal models, type of cells and TME (48,49). Nuclear βarr1 was recently shown to induce metabolic reprogramming of PCa cells which drives the expression of tumor-specific phenotypes including anchorage-independent growth, migration, invasion and proliferation (50). These data, together with the pleiotropic effects of βarr1 on GPCR-mediated cellular functions, suggest that further studies using different models of PCa are required for the complete understanding of βarr1 effect in prostate tumorigenesis.

Supplementary material

Supplementary data are available at *Carcinogenesis* online.

Supplementary Figure S1. βarr1 and βarr2 expression in PCa cells. RT-PCR analysis of βarr1 (**A**) and βarr2 (**B**) expression in AA (MDA PCa 2b and E006AA) and CA (LNCaP and PC3) relative to normal prostate cells (RWPE-1). Data shown are from three experiments carried out in triplicate. $^{**}P < 0.01$; $^{***}P < 0.001$. For western blot analysis of βarr1 (**C**) and βarr2 (**E**) expression in PCa cells, cell lysates (20 µg of proteins) were resolved on a 10% SDS-PAGE, transferred to nitrocellulose paper and probed with anti-βarr1 or anti-βarr2 antibodies. Band density was calculated by ImageJ software, normalized for GAPDH expression and are the averages of three experiments (**D**) and (**F**) $^{*}P < 0.05$; $^{**}P < 0.005$; $^{***}P < 0.001$.

Supplementary Figure S2. Overexpression of βarr2 in PC-3 and LNCaP cells had no significant effect in tumor development. (**A**) PC-3 cells were stably transfected with pcDNA3-EGFP or pCDNA3-EGFP expressing β-arrestin 2 (pCDNA3-βarr2-GFP) and overexpression of βarr2 was assessed by immunoblotting. Cells (5×10^6 cells) were injected in 6-week-old nude mice. Twenty-eight days post-injection mice were euthanized, tumors were excised and tumor weights were determined. (**B**) LNCaP cells were stably transfected with pCDNA3-EGFP or pCDNA3-EGFP expressing β-arrestin 2 (pCDNA3-βarr2-GFP) and overexpression of βarr2 was assessed by immunoblotting. Cells (5×10^6 cells) were injected in 6-week-old nude mice. Six weeks post-injection mice were euthanized, tumors were excised and tumor weights were determined. Data shown are representative of two independent experiments.

Supplementary Figure S3. βarr1 and βarr2 expression in TRAMP, TRAMP/βarr1$^{-/-}$ and TRAMP/βarr2$^{-/-}$ prostate tumors. Tissue sections from TRAMP, TRAMP/βarr1$^{-/-}$ and TRAMP/βarr2$^{-/-}$ prostate tumors were immunostained with anti-βarr1 and anti-βarr2 antibodies. Representative images of two independent experiments are shown. Scale bars: 50 µm.

Acknowledgements

We thank Dr Robert J. Lefkowitz (Howard Hughes Medical Institute, Duke University Medical Center, Durham, NC) for providing the βarr1$^{-/-}$ and βarr2$^{-/-}$ mice. We are very thankful to Ms Tonelia Mowart (Department of Biomedical and Biological Science and JLC Biomedical/Biotechnology Research Institute, NCCU, Durham, NC) for her technical support.

Funding

This work was supported by National Institutes of Health grants (AI38910, CA156735, MD012392) and USAMRMC grant W81XWH-07-1-0418.

Conflict of Interest Statement: None declared.

References

1. Siegel, R.L. *et al.* (2020) Cancer statistics, 2020. *CA Cancer J. Clin.*, 70, 7–30.
2. Welch, H.G. *et al.* (2009) Prostate cancer diagnosis and treatment after the introduction of prostate-specific antigen screening: 1986-2005. *J. Natl. Cancer Inst.*, 101, 1325–1329.
3. Thompson, I.M. *et al.* (2006) Assessing prostate cancer risk: results from the Prostate Cancer Prevention Trial. *J. Natl. Cancer Inst.*, 98, 529–534.
4. Du, X.L. *et al.* (2006) Racial disparity and socioeconomic status in association with survival in older men with local/regional stage prostate carcinoma: findings from a large community-based cohort. *Cancer*, 106, 1276–1285.
5. Gilligan, T. (2005) Social disparities and prostate cancer: mapping the gaps in our knowledge. *Cancer Causes Control*, 16, 45–53.
6. Hayes, R.B. *et al.* (1999) Dietary factors and risks for prostate cancer among blacks and whites in the United States. *Cancer Epidemiol. Biomarkers Prev.*, 8, 25–34.
7. Bratt, O. (2002) Hereditary prostate cancer: clinical aspects. *J. Urol.*, 168, 906–913.
8. Marks, L.S. *et al.* (2006) Prostatic tissue testosterone and dihydrotestosterone in African-American and white men. *Urology*, 68, 337–341.
9. Powell, I.J. *et al.* (2013) Genes associated with prostate cancer are differentially expressed in African American and European American men. *Cancer Epidemiol. Biomarkers Prev.*, 22, 891–897.
10. Winters, S.J. *et al.* (2001) Testosterone, sex hormone-binding globulin, and body composition in young adult African American and Caucasian men. *Metabolism*, 50, 1242–1247.
11. Gaston, K.E. *et al.* (2003) Racial differences in androgen receptor protein expression in men with clinically localized prostate cancer. *J. Urol.*, 170, 990–993.
12. Shen, H. *et al.* (2006) The Duffy antigen/receptor for chemokines (DARC) regulates prostate tumor growth. *FASEB J.*, 20, 59–64.
13. Benovic, J.L. *et al.* (1987) Functional desensitization of the isolated beta-adrenergic receptor by the beta-adrenergic receptor kinase: potential role of an analog of the retinal protein arrestin (48-kDa protein). *Proc. Natl. Acad. Sci. USA*, 84, 8879–8882.
14. Hausdorff, W.P. *et al.* (1990) Turning off the signal: desensitization of beta-adrenergic receptor function. *FASEB J.*, 4, 2881–2889.
15. Smith, J.S. *et al.* (2016) The β-arrestins: multifunctional regulators of G protein-coupled receptors. *J. Biol. Chem.*, 291, 8969–8977.
16. Buchanan, F.G. *et al.* (2006) Emerging roles of beta-arrestins. *Cell Cycle*, 5, 2060–2063.
17. DeWire, S.M. *et al.* (2007) Beta-arrestins and cell signaling. *Annu. Rev. Physiol.*, 69, 483–510.
18. Lakshmikanthan, V. *et al.* (2009) Identification of βArrestin2 as a corepressor of androgen receptor signaling in prostate cancer. *Proc. Natl. Acad. Sci. USA*, 106, 9379–9384.
19. Purayil, H.T. *et al.* (2015) Arrestin2 modulates androgen receptor activation. *Oncogene*, 34, 3144–3151.
20. Raghuwanshi, S.K. *et al.* (2008) Depletion of β-arrestin-2 promotes tumor growth and angiogenesis in a murine model of lung cancer. *J. Immunol.*, 180, 5699–5706.
21. Scudiero, D.A. *et al.* (1988) Evaluation of a soluble tetrazolium/formazan assay for cell growth and drug sensitivity in culture using human and other tumor cell lines. *Cancer Res.*, 48, 4827–4833.
22. Adekoya, T.O. *et al.* (2019) Activator of G protein signaling 3 modulates prostate tumor development and progression. *Carcinogenesis*, 40, 1504–1513.
23. Greenberg, N.M. *et al.* (1995) Prostate cancer in a transgenic mouse. *Proc. Natl. Acad. Sci. USA*, 92, 3439–3443.

24. Gingrich, J.R. *et al.* (1996) Metastatic prostate cancer in a transgenic mouse. *Cancer Res.*, 56, 4096–4102.
25. Greenberg, N.M. (1996) Transgenic models for prostate cancer research. *Urol. Oncol.*, 2, 119–122.
26. Gingrich, J.R. *et al.* (1996) A transgenic mouse prostate cancer model. *Toxicol. Pathol.*, 24, 502–504.
27. Foster, B.A. *et al.* (1997) Characterization of prostatic epithelial cell lines derived from transgenic adenocarcinoma of the mouse prostate (TRAMP) model. *Cancer Res.*, 57, 3325–3330.
28. Adekoya, T.O. *et al.* (2020) Cytokines and chemokines as mediators of prostate cancer metastasis. *Int. J. Mol. Sci.*, 21, 4449.
29. Hinshaw, D.C. *et al.* (2019) The tumor microenvironment innately modulates cancer progression. *Cancer Res.*, 79, 4557–4566.
30. Bagnato, A. *et al.* (2019) New routes in GPCR/β-arrestin-driven signaling in cancer progression and metastasis. *Front. Pharmacol.*, 10, 114.
31. Zhang, L. *et al.* (2003) Intratumoral T cells, recurrence, and survival in epithelial ovarian cancer. *N. Engl. J. Med.*, 348, 203–213.
32. Yang, Y. *et al.* (2021) High intratumoral $CD8^+$ T-cell infiltration is associated with improved survival in prostate cancer patients undergoing radical prostatectomy. *Prostate*, 81, 20–28.
33. Niu, Y. *et al.* (2008) Androgen receptor is a tumor suppressor and proliferator in prostate cancer. *Proc. Natl. Acad. Sci. USA*, 105, 12182–12187.
34. Shiota, M. *et al.* (2011) Androgen receptor cofactors in prostate cancer: potential therapeutic targets of castration-resistant prostate cancer. *Curr. Cancer Drug Targets*, 11, 870–881.
35. van de Wijngaart, D.J. *et al.* (2012) Androgen receptor coregulators: recruitment via the coactivator binding groove. *Mol. Cell. Endocrinol.*, 352, 57–69.
36. Kidwai, N. *et al.* (2004) Expression of androgen receptor and prostate-specific antigen in male breast carcinoma. *Breast Cancer Res.*, 6, R18–R23.
37. Oettgen, P. *et al.* (2000) PDEF, a novel prostate epithelium-specific Ets transcription factor, interacts with the androgen receptor and activates prostate-specific antigen gene expression. *J. Biol. Chem.*, 275, 1216–1225.
38. Wang, C. *et al.* (2003) Identification of a novel transcription factor, GAGATA-binding protein, involved in androgen-mediated expression of prostate-specific antigen. *J. Biol. Chem.*, 278, 32423–32430.
39. Oettgen, P. *et al.* (1999) Characterization of ESE-2, a novel ESE-1-related Ets transcription factor that is restricted to glandular epithelium and differentiated keratinocytes. *J. Biol. Chem.*, 274, 29439–29452.
40. Kang, J. *et al.* (2005) A nuclear function of beta-arrestin1 in GPCR signaling: regulation of histone acetylation and gene transcription. *Cell*, 123, 833–847.
41. Kong, Z. *et al.* (2018) β-arrestin1-mediated inhibition of FOXO3a contributes to prostate cancer cell growth *in vitro* and *in vivo*. *Cancer Sci.*, 109, 1834–1842.
42. Uzgare, A.R. *et al.* (2003) Differential expression and/or activation of P38MAPK, erk1/2, and jnk during the initiation and progression of prostate cancer. *Prostate*, 55, 128–139.
43. Rodríguez-Berriguete, G. *et al.* (2012) MAP kinases and prostate cancer. *J. Signal Transduct.*, 2012, 169170.
44. Malik, S.N. *et al.* (2002) Immunohistochemical demonstration of phospho-Akt in high Gleason grade prostate cancer. *Clin. Cancer Res.*, 8, 1168–1171.
45. Gioeli, D. *et al.* (1999) Activation of mitogen-activated protein kinase associated with prostate cancer progression. *Cancer Res.*, 59, 279–284.
46. Pissimissis, N. *et al.* (2009) The glutamatergic system expression in human PC-3 and LNCaP prostate cancer cells. *Anticancer Res.*, 29, 371–377.
47. Engl, T. *et al.* (2006) Prostate tumor CXC-chemokine profile correlates with cell adhesion to endothelium and extracellular matrix. *Life Sci.*, 78, 1784–1793.
48. Sobolesky, P.M. *et al.* (2013) The role of β-arrestins in cancer. *Prog. Mol. Biol. Transl. Sci.*, 118, 395–411.
49. Hu, S. *et al.* (2013) Involvement of β-arrestins in cancer progression. *Mol. Biol. Rep.*, 40, 1065–1071.
50. Zecchini, V. *et al.* (2014) Nuclear ARRB1 induces pseudohypoxia and cellular metabolism reprogramming in prostate cancer. *EMBO J.*, 33, 1365–1382.